UDC 615.011:54.057:615.214.2
DOI: 10.15587/2519-4852.2025.346823

ACETYLCHOLINESTERASE-TARGETED BIOGENIC–THIENOPYRIMIDINE HYBRIDS: DESIGN, SYNTHESIS AND PHARMACOLOGICAL EVALUATION OF COMPOUNDS WITH ANTI-AMNESTIC, ANXIOLYTIC-LIKE AND PAIN-MODULATING PROPERTIES

Rita Saifudinova, Sergiy Vlasov, Hanna Severina, Georgiy Yakovenko, Andrii Khairulin, Dmytro Kyrylov, Mykyta Hutorka, Sergii Shtrygol', Victoriya Georgiyants

The aim. *To carry out the rational design, synthesis, and experimental evaluation of new glycine-linked thieno[2,3-d]pyrimidine hybrids as potential modulators of memory, anxiety, and pain for further correction of neurodegenerative processes, integrating in silico and in vivo investigations.*

Materials and methods. *Organic synthesis methods; structure confirmation by ^{1}H, ^{13}C NMR spectroscopy, LC-MS, and elemental analysis. Molecular docking was performed using AutoDock Vina, AutoDockTools 1.5.6, and Discovery Studio Client. The pharmacological studies were carried out using a scopolamine-induced amnesia model and included the following behavioral assays: the Passive Avoidance Test, the Light-dark Transition Test, the Rotarod Test, and the Hot Plate Test.*

Results and discussion. *A series of newly designed glycine-linked thieno[2,3-d]pyrimidine hybrids was rationally developed, synthesized, and evaluated as potential modulators of neurodegenerative processes. The synthetic procedures for obtaining the intermediates and target 5-methylthieno[2,3-d]pyrimidin-4(3H)-one hybrids via amide coupling were optimized. Molecular docking to AChE (PDB ID: 7E3H) revealed that several derivatives, particularly* ***4d****,* ***4f****, and* ***4g****, exhibited favorable binding energies (down to –12.5 kcal/mol) and formed an extensive network of hydrogen-bonding, halogen, π–π, and hydrophobic interactions within the active site of acetylcholinesterase. In vivo studies using the scopolamine-induced amnesia model demonstrated that these compounds display moderate anti-amnestic (pro-cognitive) properties and do not influence motor coordination or nociceptive sensitivity. Compound* ***4g*** *showed anti-amnestic activity comparable to that of Donepezil, as well as pronounced anxiolytic effects. A correlation between the in-silico predictions and the in vivo findings was established.*

Conclusions. *The rational design, synthesis, and structural characterization of new AChE-targeted inhibitors, combined with in silico calculations and subsequent in vivo validation, enabled the identification of several thieno[2,3-d]pyrimidine derivatives with moderate anti-amnestic properties in the scopolamine-induced amnesia model, highlighting their potential as promising structures for further optimization*

Keywords: *thienopyrimidine, neurodegeneration, acetylcholinesterase, glycine, amnesia*

How to cite:
Saifudinova, R., Vlasov, S., Severina, H., Yakovenko, G., Khairulin, A., Kyrylov, D., Hutorka, M., Shtrygol', S., Georgiyants, V. (2025). Acetylcholinesterase-targeted biogenic–thienopyrimidine hybrids: design, synthesis and pharmacological evaluation of compounds with anti-amnestic, anxiolytic-like and pain-modulating properties. ScienceRise: Pharmaceutical Science, 6 (58), 14–27. http://doi.org/10.15587/2519-4852.2025.346823

1. Introduction

Memory impairment is one of the leading clinical symptoms observed across a wide range of nervous and mental illnesses. These disturbances are particularly prominent in neurodegenerative diseases, where cognitive decline, including deficits in mnemonic functions, represents a key indicator of progressive damage to the central nervous system [1, 2]. Cognitive decline in these conditions is not always isolated. It is often associated with increased anxiety [3], and is also accompanied by pain syndromes [4], significantly impairing daily life and eventually making independent functioning impossible. Numerous factors contribute to the development of neurodegeneration, and the significant role of amino acids in the pathogenesis of neurodegenerative disorders is a well-established scientific fact. Alterations in their metabolism, transport, and neurotransmitter functions are considered among the principal mechanisms that promote the progression of degenerative processes within the central nervous system. Accumulating evidence indicates that amino acids and their derivatives may function not only as potential biomarkers of neurodegenerative processes but also as promising therapeutic candidates for mitigating their progression [5]. Among these molecules, glycine has shown notable neuroprotective properties. In experimental models, glycine was found to suppress D-gal-induced oxidative stress and to restore the expression and immunoreactivity of key antioxidant proteins, including Nrf2 and HO-1, which were markedly reduced in the brains of treated mice [6].

The study in the CRND8 mouse model of Alzheimer's disease demonstrated that the levels of glutamate and glutamine were decreased in the hippocampus, cortex, and midbrain of the affected neurons [7]. Glutamate level for sure plays an important role in the energy metabolism as it

is the primary excitatory neurotransmitter in the brain. In course of Alzheimer's disease, the levels of alanine, aspartate, and glycine were reported to be elevated [8]. Peptides are also of considerable interest as a promising source of biologically active molecules with therapeutic potential for the treatment of neurodegenerative disorders [9]. For instance, several studies have hypothesized that the ingestion of lactotripeptides may enhance cerebral blood flow and thereby improve cognitive function [10]. Furthermore, Met-Lys-Pro (MKP), a casein-derived peptide with ACE-inhibitory properties and the potential to cross the blood-brain barrier, has been reported to mitigate cognitive decline in a mouse model of Alzheimer's disease [11].

Tryptamine is increasingly recognized as a privileged scaffold for the design of anti-neurodegenerative agents, particularly in the context of Alzheimer's disease [12]. Recent studies show that tryptamine-based hybrids exhibit therapeutic potential against cholinesterase-associated disorders, including AD and Parkinson's disease, and may serve as promising building blocks for developing multitarget-directed ligands [13]. At the same time, the melatonin motif, another indole-derived structural element, is widely utilized in the design of neuroprotective molecules due to its inherent antioxidant and anti-inflammatory properties, making it a valuable fragment for creating compounds aimed at mitigating neurodegenerative processes [14].

Biogenic molecules are often used as key building blocks for the development of drug candidates against neurodegeneration, since they provide favorable biological properties and naturally interact with neuronal pathways [15, 16]. Based on such fragments, the strategy of synthetic-biogenic hybridization has been increasingly explored, as it allows the combination of natural structural elements with synthetic pharmacophores to obtain multitarget molecules. The potential of this approach is supported by cinnamoyl N-acylhydrazone donepezil hybrids, which have demonstrated significant activity in neurodegeneration models [17]. Additional examples include hybrids of β-phenylacrylic acid with methyl esters of natural amino acids that showed pronounced anti neuroinflammatory effects [18], as well as other amino acid containing hybrids that influence key pathogenic mechanisms of neurodegenerative disorders [19]. Peptoids, which are N substituted glycine derivatives, also attract considerable interest because they exhibit enhanced stability and confirmed neuroprotective potential [20].

Thienopyrimidine derivatives have attracted considerable attention as promising scaffolds in medicinal chemistry due to their structural flexibility and ability to interact with a broad range of biological targets [21]. A number of studies have demonstrated their potential in the treatment of neurodegenerative diseases, particularly through multimodal mechanisms that include cholinesterase inhibition, antioxidant activity, and modulation of amyloidogenic pathways [21, 23]. Additional interest in this class of heterocycles is supported by the development of compounds with complex neuromodulatory activity, such as DDP-225, which combines norepinephrine reuptake inhibition with 5-HT_3 receptor antagonism and has been investigated in the context of cognitive and neurodegenerative disorders [24]. Collectively, these findings indicate that thienopyrimidines represent a promising platform for the development of new multitarget agents capable of modulating key pathogenic pathways involved in neurodegeneration.

The aim of the research. The aim of this study is the rational design, synthesis, and experimental evaluation of new glycine-linked thieno[2,3-d]pyrimidine hybrids as potential modulators of memory, anxiety, and pain for further correction of neurodegenerative processes, integrating *in silico* and *in vivo* investigations.

2. Planning (methodology) of research

To achieve the stated goal, we carried out the design of new derivatives using a pharmacophore-based approach, followed by synthesis and structural analysis of the target compounds, as well as targeted virtual screening against the therapeutically relevant target AChE, which is important for assessing potential effects on underlying cognitive disorders. Subsequent *in vivo* screening of the most promising structures provided experimental verification of their potential pro-cognitive activity, enabling the identification of compounds suitable for further optimization.

At the design stage the thieno[2,3-d]pyrimidine scaffold modified with a glycine linker at position 3 was selected as the core structure (Fig. 1). Subsequent design steps involved the incorporation of biogenic and synthetic fragments relevant to major neurotransmitter systems and pathogenic mechanisms implicated in neurodegeneration.

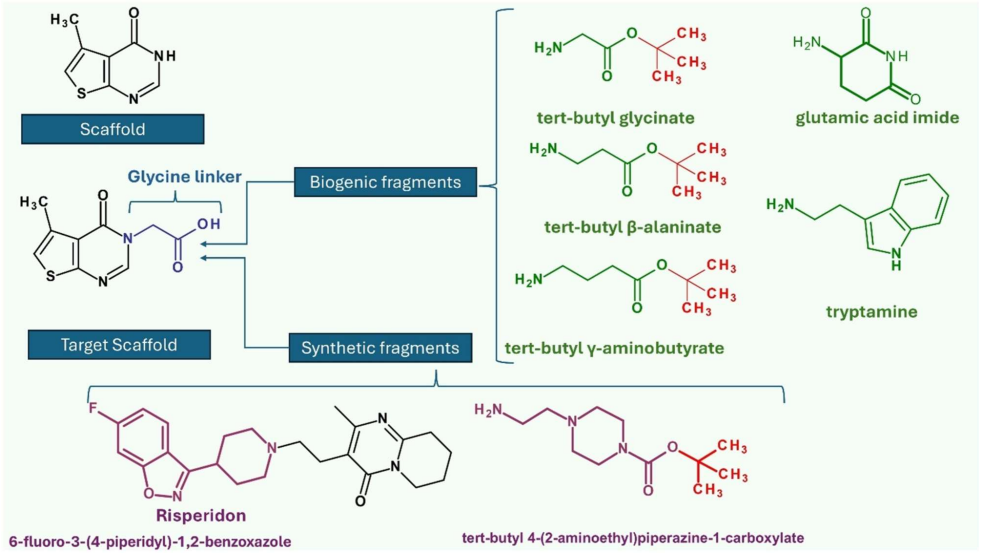

Fig. 1. Overall design concept for the synthesized hybrid molecules

Tert-butyl esters of glycine, β-alanine, and γ-aminobutyric acid were chosen as masked forms of CNS inhibitory amino acids, providing controlled release and potential modulation of inhibitory neurotransmission. The selection of *tert*-butyl esters was guided by their reduced polarity and increased lipophilicity, which enhance the ability of molecules to cross the BBB a critical property for CNS-oriented drug candidates [25]. Additionally, conflicting data regarding the influence of *tert*-butyl substituents on metabolic stability further motivated their inclusion: some studies suggest that *tert*-butyl groups exhibit low metabolic stability [26], whereas others report that replacing an isopropyl group with a *tert*-butyl moiety in the ester function can improve metabolic stability of drug candidates [27]. Testing this series allowed us to explore these contrasting observations. The imide of glutamic acid was incorporated as a cyclized form of the excitatory neurotransmitter, providing increased stability, enhanced lipophilicity, and better suitability for integration into hybrid molecules compared with the free amino acid. Tryptamine was included owing to its established activity toward serotonergic and dopaminergic systems, dysfunction of which is characteristic of many neurodegenerative disorders.

Among the synthetic components, the protected 2-(piperazin-1-yl)ethanamine fragment was selected as a representative aliphatic amine with a favorable interaction profile toward biologically relevant targets and as a widely used linker in the design of CNS-active compounds [28]. The 6-fluoro-3-(piperidin-4-yl)-1,2-benzoxazole fragment was chosen due to its presence in the structures of atypical antipsychotics, including risperidone and paliperidone, which modulate central neurotransmitter systems implicated in neuroprotection [29]. Such a combination of biogenic and synthetic fragments aligns with contemporary strategies in hybrid molecule design aimed at generating multifunctional ligands capable of acting on multiple therapeutic targets involved in neurodegenerative processes.

3. Materials and methods

3. 1. Chemistry

All the solvent and reagents were used from Enamine Ltd. stock without additional purification. ^{1}H NMR spectra were recorded on a Varian Unity Plus 400 (400 and 376 MHz, respectively) instrument, ^{1}H and ^{13}C NMR spectra were recorded on a Bruker 170 Avance 500 (500 and 126 MHz, respectively) instrument, ^{13}C NMR spectra were recorded also on an Agilent ProPulse 600 (151 MHz) spectrometer. The NMR chemical shifts are referenced using the solvent signals at 7.26 and 77.1 ppm for ^{1}H and ^{13}C nuclei, respectively, in $CDCl_3$ and 2.48 and 39.5 ppm for ^{1}H and ^{13}C nuclei, respectively, in DMSO-d_6. Mass spectra were obtained on an Agilent LC/MSD SL 1100 instrument (atmospheric pressure electrospray ionization (ES-API)). Melting points were measured in open capillary tubes and are given uncorrected.

The starting 5-methylthieno[2,3-*d*]pyrimidin-4(3*H*)-one **1** [30] was obtained from ethyl 2-amino-4-methylthiophene-3-carboxylate by boiling in foramimide [31, 32].

Ethyl (5-methyl-4-oxothieno[2,3-d]pyrimidin-3(4H)-yl)acetate (2) [33].

To 13.5 g (0.08 mol) of 5-methylthieno[2,3-*d*]pyrimidin-4(3H)-one 1 dissolved in 55 mL of dimethylformamide, 12.2 g (0.09 mol) of potassium carbonate and 10.85 mL (0.10 mol) of ethyl bromoacetate were added. After the addition of a catalytic amount of potassium iodide, the reaction mixture was heated at 65°C for 12 hours. The progress of the reaction was monitored by LC–MS. Upon completion, the mixture was cooled to room temperature, and the resulting precipitate was filtered off. The filtrate was then slowly quenched with distilled water under stirring until crystallization began. After the crystals formed (within 5–7 minutes), they were filtered and washed with water. If necessary, the product was further purified by crystallization from ethanol. Yield 72%, a white powder; mp 128–130°C; ^{1}H NMR (400 MHz, DMSO-d_6) δ 8.33 (s, 1H), 7.18 (*s*, 1H), 4.76 (s, 2H), 4.14 (*q*, J = 7.1 Hz, 2H), 2.42 (*s*, 3H), 1.19 (*t*, J = 7.1 Hz, 3H). ^{13}C NMR (126 MHz, DMSO-d_6) δ 168.3, 164.4, 157.8, 148.7, 134.1, 122.25, 119.7, 71.1, 61.7, 47.3, 16.5, 14.4. LC-MS, *m/z*: 253 $[M+H]^+$. Anal. Calcd for $C_{11}H_{12}N_2O_3S$ (M.w. 252.29): C, 52.37; H, 4.79; N, 11.10. Found: C, 52.37; H, 4.82; N, 11.10.

(5-Methyl-4-oxothieno[2,3-d]pyrimidin-3(4H)-yl) acetic acid (3).

To 15.0 g (0.06 mol) of ester **2**, 8.0 g (0.2 mol) of dry sodium hydroxide was added, and the reaction mixture (water–methanol, 1:1; 150 mL) was heated under reflux for 1–2 hours. The progress of the reaction was monitored by LC–MS. After completion, the mixture was cooled and acidified with hydrochloric acid to pH 3. The resulting precipitate of the acid **3** was filtered, washed thoroughly with water, and dried at 60°C. Yield 52%, a white powder; mp 283°C; ^{1}H NMR (500 MHz, DMSO-d_6) δ 13.22 (*s*, 1H), 8.34 (*s*, 1H), 7.18 (*s*, 1H), 4.69 (*s*, 2H), 2.44 (*s*, 3H). ^{13}C NMR (126 MHz, DMSO-d_6) δ 169.6, 164.4, 157.8, 148.8, 134.1, 122.2, 119.5, 47.2, 16.5. LC-MS, *m/z*: 225 $[M+H]^+$. Anal. Calcd for $C_9H_8N_2O_3S$ (M.w. 224.24): C, 48.21; H, 3.60; N, 12.49. Found: C, 48.28; H, 3.71; N, 12.59.

General method of coupling of (5-methyl-4-oxothieno[2,3-d]pyrimidin-3(4H)-yl)acetic acid 3.

The acid 3 0.2 g (0.0009 mol) was mixed with 0.144 g (0.001 mol) of 1,1'-carbonyldiimidazole and to the mixture 4 ml of anhydrous 1,4-dioxane was added. The reaction mixture was heated at 80-90^{0}C with stirring and protected from the contact with the air by the gas bubbler filled with 1,4-dioxane. The reaction mixture was heated till the clear solution is formed and then additionally for 15 minutes to let all the carbon dioxide be released. Then the reaction mixture was cooled and 0.001 mole of the correspondent amine or its hydrochloride was added. In the case of hydrochlorides 0.001 mole of triethylamine was added to the reaction mixture. The reaction mixture was heated and stirred at the same temperature for 4–5 hours. The reaction progress was monitored by LC-MS. After the conversion was completed the solvent was distilled off at the reduced pressure, and the solid residue was diluted with waster to for the target

product. The analytical samples were additionally crystallized from the suitable alcohols.

tert-Butyl {[(5-methyl-4-oxothieno[2,3-d]pyrimidin-3(4H)-yl)acetyl]amino}acetate (4a).

Yield 74%, a white powder; mp 144–145°C; ^{1}H NMR (600 MHz, DMSO-d_6) δ 8.66 (*t*, *J* = 5.9 Hz, 1H), 8.27 (*s*, 1H), 7.14 (*s*, 1H), 4.67 (s, 2H), 3.78 (*d*, *J* = 5.8 Hz, 2H), 2.43 (*s*, 3H), 1.38 (*s*, 9H). ^{13}C NMR (151 MHz, DMSO-d_6) δ 169.1, 167.4, 164.4, 157.8, 149.2, 134.1, 122.2, 119.2, 81.2, 47.7, 41.8, 28.1, 16.5. LC-MS, *m/z*: 338 $[M+H]^+$. Anal. Calcd for $C_{15}H_{19}N_3O_4S$ (M.w. 337,40): C, 53.40; H, 5.68; N, 12.45. Found: C, 53.44; H, 5.72; N, 12.56.

tert-butyl 3-{[(5-methyl-4-oxothieno[2,3-d]pyrimidin-3(4H)-yl)acetyl]amino} propanoate (4b).

Yield 66%, a white powder; mp 163–165°C; ^{1}H NMR (400 MHz, DMSO-d_6) δ 8.34 (*t*, *J* = 5.6 Hz, 1H), 8.23 (*s*, 1H), 7.13 (*s*, 1H), 4.56 (*s*, 2H), 3.25 (*q*, *J* = 6.4 Hz, 2H), 2.41 (*s*, 3H), 2.35 (*t*, *J* = 6.7 Hz, 2H), 1.37 (s, 9H). ^{13}C NMR (126 MHz, DMSO-d_6) δ 170.9, 167.0, 164.4, 157.9, 149.3, 134.1, 122.3, 119.2, 80.4, 47.9, 35.5, 35.3, 28.2, 16.6. LC-MS, *m/z*: 296 $[M-(CH_3)_3C]^+$. Anal. Calcd for $C_{16}H_{21}N_3O_4S$ (M.w. 351,43): C, 54.69; H, 6.02; N, 11.96. Found: C, 54.71; H, 6.10; N, 12.07.

tert-butyl 4-{[(5-methyl-4-oxothieno[2,3-d]pyrimidin-3(4H)-yl)acetyl]amino}butanoate (4c).

Yield 81%, a white powder; mp 153–155°C; ^{1}H NMR (400 MHz, DMSO-d_6) δ 8.25 (*br.s*, 2H), 7.13 (*s*, 1H), 4.56 (*s*, 2H), 3.06 (*q*, *J* = 6.5 Hz, 2H), 2.41 (*s*, 3H), 2.19 (*t*, *J* = 7.5 Hz, 2H), 1.60 (*p*, *J* = 7.2 Hz, 2H), 1.35 (*s*, 9H). ^{13}C NMR (126 MHz, DMSO-d_6) δ 172.3, 166.8, 164.4, 157.9, 149.3, 134.1, 122.3, 119.1, 80.0, 48.1, 38.5, 32.6, 28.2, 25.1, 16.6.

LC-MS, *m/z*: 310 $[M-(CH_3)_3C]^+$. Anal. Calcd for $C_{17}H_{23}N_3O_4S$ (M.w. 365,45): C, 55.87; H, 6.34; N, 11.50. Found: C, 56.01; H, 6.37; N, 11.60.

N-(2,6-Dioxopiperidin-3-yl)-2-(5-methyl-4-oxothieno[2,3-d]pyrimidin-3(4H)-yl)acetamide (4d).

Yield 75%, a white powder; mp > 250°C; ^{1}H NMR (400 MHz, DMSO-d_6) δ 10.82 (*s*, 1H), 8.67 (*d*, *J* = 8.0 Hz, 1H), 8.27 (*s*, 1H), 7.14 (*s*, 1H), 4.79–4.49 (*m*, 3H), 2.70 (*ddd*, *J* = 18.0, 12.4, 6.0 Hz, 1H), 2.42 (*s*, 3H), 1.91 (*dqd*, *J* = 17.4, 12.8, 10.4, 4.2 Hz, 2H).^{13}C NMR (126 MHz, DMSO-d_6) δ 173.2, 172.2, 167.1, 164.4, 157.9, 149.2, 134.1, 122.3, 119.2, 49.8, 47.8, 31.2, 24.8, 16.6.

LC-MS, *m/z*: 335 $[M+H]^+$. Anal. Calcd for $C_{14}H_{14}N_4O_4S$ (M.w. 334,36): C, 50.29; H, 4.22; N, 16.76. Found: C, 50.27; H, 5.36; N, 16.80.

tert-Butyl 4-(2-{[(5-methyl-4-oxothieno[2,3-d]pyrimidin-3(4H)-yl)acetyl]amino}ethyl)piperazine-1-carboxylate (4e).

Yield 64%, a white powder; mp 179–180°C; ^{1}H NMR (400 MHz, DMSO-d_6) δ 8.24 (s, 1H), 8.22 (*d*, *J* = 6.4 Hz, 1H), 7.13 (*s*, 1H), 4.58 (s, 2H), 3.26 (*d*, *J* = 10.0 Hz, 3H), 3.18 (*q*, *J* = 6.5 Hz, 2H), 2.41 (*s*, 3H), 2.32 (*dt*, *J* = 17.8, 6.0 Hz, 6H), 1.35 (*s*, 9H).^{13}C NMR (126 MHz, *DMSO-d_6*) *δ* 166.9, 164.4, 157.9, 154.2, 149.3, 134.1, 122.3, 119.2, 79.1, 57.2, 52.9, 48.0, 36.8, 28.5, 16.6. LC-MS, m/z: 436 $[M+H]^+$. Anal. Calcd for $C_{20}H_{29}N_5O_4S$ (M.w. 435.55): C, 55.15; H, 6.71; N, 16.08. Found: C, 55.22; H, 6.71; N, 16.09.

N-[2-(1H-indol-3-yl)ethyl]-2-(5-methyl-4-oxothieno[2,3-d]pyrimidin-3(4H)-yl)acetamide (4f).

Yield 84%, a white powder; mp 228–230°C; ^{1}H NMR (400 MHz, DMSO-d_6) δ 10.81 (*s*, 1H), 8.42 (*t*, *J* = 5.6 Hz, 1H), 8.26 (*s*, 1H), 7.51 (*d*, *J* = 7.9 Hz, 1H), 7.32 (*d*, *J* = 8.0 Hz, 1H), 7.22–7.10 (*m*, 2H), 7.04 (*t*, *J* = 7.5 Hz, 1H), 6.95 (*t*, *J* = 7.4 Hz, 1H), 4.61 (*s*, 2H), 3.36 (*q*, *J* = 6.9 Hz, 2H), 2.83 (*t*, *J* = 7.5 Hz, 2H), 2.44 (*s*, 3H). ^{13}C NMR (151 MHz, DMSO-d_6) δ 166.8, 164.4, 157.9, 149.3, 136.6, 134.1, 127.6, 123.2, 122.3, 121.3, 119.1, 118.7, 118.6, 112.0, 111.8, 48.0, 25.5, 16.6. LC-MS, *m/z*: 367 $[M+H]^+$.

Anal. Calcd for $C_{19}H_{18}N_4O_2S$ (M.w. 366,44): C, 62.28; H, 4.95; N, 15.29. Found: C, 62.55; H, 5.05; N, 15.30.

3-{2-[4-(6-fluoro-1,2-benzoxazol-3-yl)piperidin-1-yl]-2-oxoethyl}-5-methylthieno[2,3-d]pyrimidin-4(3H)-one (4g).

Yield 87%, a white powder; mp 208 – 209°C; ^{1}H NMR (400 MHz, DMSO-d_6) δ 8.24 (*s*, 1H), 8.04 (*dd*, *J* = 8.9, 5.0 Hz, 1H), 7.75–7.61 (*m*, 1H), 7.26 (*td*, *J* = 9.2, 2.3 Hz, 1H), 7.15 (*s*, 1H), 4.94 (*s*, 2H), 4.36 (*d*, *J* = 13.0 Hz, 1H), 4.07 (d, *J* = 13.8 Hz, 1H), 3.60–3.40 (*m*, 2H), 3.31 (*p*, *J* = 13.6, 12.9 Hz, 2H), 2.89 (*t*, *J* = 12.1 Hz, 1H), 2.20–2.02 (m, 2H), 1.93 (*q*, *J* = 12.8, 12.0 Hz, 1H), 1.67 (*tt*, *J* = 13.1, 6.5 Hz, 1H).^{13}C NMR (126 MHz, DMSO-d_6) δ 165.2, 165.1, 164.4, 163.6, 163.5, 163.1, 161.3, 157.9, 149.3, 137.5, 134.1, 129.2, 124.2, 124.2, 122.3, 119.2, 119.0, 117.5, 113.1, 112.9, 97.9, 97.7, 66.8, 46.6, 46.1, 44.7, 42.1, 33.5, 33.4, 30.5, 30.1, 29.9, 16.6. LC-MS, *m/z*: 427 $[M+H]^+$. Anal. Calcd for $C_{21}H_{19}FN_4O_3S$ (M.w. 426,47): C, 59.14; H, 4.49; N, 13.14. Found: C, 59.18; H, 4.58; N, 13.25.

3. 2. Molecular docking studies

Flexible molecular docking was employed to evaluate the affinity of the designed molecules toward selected biological targets. Protein structures were retrieved from the Protein Data Bank [34]. Acetylcholinesterase from *Homo sapiens* (PDB ID: 7E3H) [35], with donepezil as a native ligand, was used for the docking experiments. The grid box parameters were defined as follows: center_x = –43.368, center_y = 37.728, center_z = –30.313; size_x = 38, size_y = 22, size_z = 28.

Ligand structures were generated in BioviaDraw 2021 and exported in MOL format. Geometry optimization was performed in Chem3D using the MM2 molecular mechanics algorithm to yield PDB files. The use of MM2 provided refined geometries due to its extensive parameterization for organic molecules. The optimized structures were converted to PDBQT format in AutoDockTools 1.5.6 with default torsional settings. Protein structures were prepared by removing water molecules and co-crystallized ligands in Discovery Studio, followed by saving the cleaned models as PDB files. Polar hydrogens were added in AutoDockTools 1.5.6, and the proteins were further converted to PDBQT format for docking. Docking simulations were carried out using AutoDock Vina, and the resulting binding poses were visualized and analyzed with Discovery Studio v19.1.0.18287.

The docking protocol was validated by re-docking the reference ligand donepezil into the active site of AChE. The calculated RMSD between the experimental

and re-docked conformations was 0.089 Å, confirming high reliability and reproducibility of the docking model.

3. 3. Pharmacological activity experiment (in vivo studies)

Experimental animals. A cohort of 42 adult random-bred male albino mice weighing about 30 g were used for the study in PAT. The animals were obtained from the vivarium of the Central Research Laboratory (National University of Pharmacy, Kharkiv, Ukraine). Experiments were performed in accordance with „Directive 2010/63/EU of the European Parliament and of the Council of 22 September 2010 on the protection of animals used for scientific purposes“ [36] and approved by the Bioethics Committee of National University of Pharmacy (excerpt from the meeting protocol No. 17 dated March 05, 2025). The animals were housed in standard polypropylene cages and kept at 22±2 ºC and 60% humidity in a well-ventilated room with a 12 h light/dark cycle with free access to food and water [37].

Animals and grouping. Animals were randomized into seven groups (n = 6). Group 1 (Vehicle control, VC): received water i.g. 20–30 min before i.p. saline and 30 min before passive avoidance training. Group 2 (Amnesia control, AC): received saline i.g., followed 30 min later by scopolamine (1.5 mg/kg, i.p.), 20–30 min before training. Group 3 (Donepezil): received donepezil suspension (3.0 mg/kg, i.g.) 30 min before scopolamine and 20–30 min before training. Animals in Groups 4–7 received water suspensions of the test compounds (stabilized with Tween-80) 30 min before scopolamine (1.5 mg/kg, i.p.) and 20–30 min before training: Group 4 – compound **4d** (2.64 mg/kg, i.g.), Group 5 – compound **4e** (3.44 mg/kg, i.g.), Group 6 – compound **4f** (2.90 mg/kg, i.g.), Group 7 – compound **4g** (3.37 mg/kg, i.g.). No adverse effects were observed in animals treated with compounds **4d, 4e, 4f, 4g** or with the reference drug. General condition, motor activity and appearance remained normal; fur was smooth and mucous membranes retained of natural pink coloration.

Reference drug (Donepezil) and preparation of formulations. Donepezil (Alzepil®*, Egis, Hungary*) was administered at a dose equivalent to 3 *mg*/kg of pure Donepezil [38]. The tablets were ground in a mortar and suspended in distilled water containing Tween-80. Suspensions of the test compounds **4a–g** were prepared analogously and stabilized with Tween-80. The doses of compounds **4a–g** were adjusted to be equimolar to the Donepezil dose (Table A), which ensured appropriate comparability of pharmacological effects. The volume of all administered suspensions (Donepezil, test compounds, or water) was calculated as 0.1 mL per 10 g of body mass for intragastric administration.

Protocol of the research. The screening study was structured to allow assessment of all targeted activities following a single administration of the tested compound. Thirty minutes after intragastric administration of the test compound or Donepezil, the animals received scopolamine hydrobromide (i.p.). After an additional 20–30 minutes, the animals were evaluated for anxiety-like behavior and subjected to passive avoidance training (PAT). Thirty minutes later, the rotarod and hot-plate tests were performed. To assess memory formation and retrieval, the retention test for PAT was conducted 24 hours after the acquisition phase.

Passive a*voidance test.* Memory consolidation and retrieval were assessed using the passive avoidance test based on rodents' innate preference for dark spaces [39, 40]. The apparatus consists of illuminated and dark compartments separated by a sliding door, with the dark chamber equipped with an electrified grid delivering a mild foot shock (0.6 mA). During acquisition, animals were placed in the illuminated compartment and allowed to explore. When the sliding door opened, they could enter the dark compartment, where entry triggered door closure and the foot shock. The retention test was conducted 24 hours later. Animals were again placed in the illuminated compartment with the door open, and the latency to enter the dark chamber was recorded as a measure of emotional memory. Failure to enter within 3 minutes was considered successful retention (latency recorded as 180 sec)

*Modeling of amnesia and calculation of anti-amnestic activity (*AA*) index.* Anterograde amnesia was induced by i.p. administration of scopolamine hydrobromide trihydrate (Thermo Fisher Scientific, China) at a dose of 1.5 *mg*/kg, given 20–30 *min* before training [41]. Retention in the passive avoidance test was assessed 24 h later by measuring the latency to enter the dark compartment and by recording the number of animals that reached the training criterion. The anti-amnestic activity (AA) index was calculated using a modified Buttler formula*:*

$$AA = (\Delta TLD - \Delta TLAC) / (\Delta TLVC - \Delta TLAC) \times 100\ (\%),$$

where AA – anti-amnestic activity, %; ΔTLD – the change in latency of the training and retention test for the drug-treated group (substances or donepezil); $\Delta TLAC$ – the change in latency of the training and retention test for the scopolamine-treated group (amnesia control group); $\Delta TLVC$ – the change in latency of the training and retention test for the VC group.

In parallel with retention assessment, exploratory and emotional responses were evaluated. Exploratory activity was assessed by the number of unfinished attempts to enter (NUAE), defined as peeking into the dark compartment without full entry [42], as well as rearing in the light compartment as a manifestation of exploratory behavior. Emotional responses were evaluated by counting grooming episodes, while vegetative manifestations of emotional reactions were assessed by the number of fecal boli and urinations.

Assessment of anxiety-like behavior. Anxiety-like behavior was assessed using the same apparatus as in the PAT experiment, following the general principles of the light–dark transition test. The method is based on the innate aversion of mice to brightly illuminated areas and their spontaneous exploratory behavior in novel environments. The light–dark box (LDB) test is widely used for evaluating anxiety-like states in rodents and is sensitive to anxiolytic drug treatment [43, 44].

In our modified version of the LDB test, only the latency to enter the dark compartment (310 lux in the light chamber) was recorded; the number of transitions and time spent in each compartment were not measured. This simplified protocol was integrated into the first day of the PAT procedure (training phase) and was sufficient to assess anxiety levels in the experimental animals. A shorter latency to enter the dark compartment was interpreted as a higher level of anxiety [42].

Assessment of coordination and balance. Motor coordination and balance were evaluated using the rotarod test [45], a widely applied screening method for detecting neurotoxicity [46]. Mice were placed on a horizontal rotating rod set at 10 rpm and allowed to walk forward to maintain balance. Each animal underwent three trials with 5-minute intervals for adaptation. The latency to fall during the third trial was recorded, with a maximum observation period of 3 minutes.

Assessment of pain response. Pain sensitivity was evaluated using the hot plate test (Hot/Cold Plate, Bioserb, USA). Mice were placed on a heated surface maintained at 54°C with transparent side walls. The animals' behavior was observed, and the latency to hind paw licking considered the most sensitive indicator of nociceptive response was recorded [47]. If no nociceptive reaction was observed by the 60th second, the mouse was removed from the plate to prevent burns; in such cases the latency time was assumed to be 60 s.

Statistical analysis. Data were processed using MS Excel 2016 and STATISTICA v.12. The Shapiro-Wilk test was applied to assess data distribution. Since the distribution was non-normal, differences between independent groups were evaluated using the Kruskal-Wallis test, followed by the Mann–Whitney U post-hoc test to identify pairwise differences. Results are presented as medians with 25% and 75% percentiles (Me [Q25; Q75]), arithmetic means with standard errors ($M \pm m$), or percentages. For binary (presence/absence) variables, Fisher's z-transformation was used. Differences were considered statistically significant at $p < 0.05$.

4. Results

The key intermediate in our strategy of building of hybrid molecules was 5-methyl-4-oxothieno[2,3-d]pyrimidin-3(4H)-yl)acetic acid, for purpose of which synthesis we optimized the alkyaltion of 5-methylthieno[2,3-*d*]pyrimidin-4(3*H*)-one (Fig. 2). In this case we added potassium iodide to facilitate the reaction, which speeded up the reaction and increased the ratio of the desired isomer of N-alkylation in the mixture. We also improved the procedure of crystallization. The fast crystalliaztion of allowed us to isolate less soluble product of N-alkylation and not allow the other by-products to precipitate.

The further hydrolysis of the obtained ester **2** was performed in methanol-water (1:1) mixture. The suggested conditions made possible to carry out the rection homogenously and to avoid any precipitation of by-products during the isolation of the acid **3**. The resulting acid **3** was thoroughly dried for use in subsequent amide coupling reactions.

Hybrid molecules **4** were obtained *via* peptide-type coupling of acid **3** with the corresponding amino acid derivatives or amines (Scheme 2). A notable advantage of this approach is that acid **3**, despite its low solubility in 1,4-dioxane, readily forms the corresponding imidazolide, which is well soluble in this solvent. Triethylamine was used in equimolar amounts *in situ* to activate the amino acid esters or amines employed in the coupling reaction in the form of hydrochlorides. Isolation of compounds **4** was also facilitated by their relatively high lipophilicity, which allowed them to be easily precipitated upon the addition of water to the reaction mixture.

Standard spectroscopic and mass-spectrometric methods were employed to confirm the structure and purity of the compound. In particular, ^{1}H and ^{13}C NMR spectroscopy was performed, allowing the identification of characteristic proton and carbon chemical shifts. Mass spectrometry (LC-MS) confirmed the molecular mass of the analyzed compound. Elemental analysis was also carried out, demonstrating a good match between the calculated and experimentally obtained composition, thus confirming the purity of the synthesized sample.

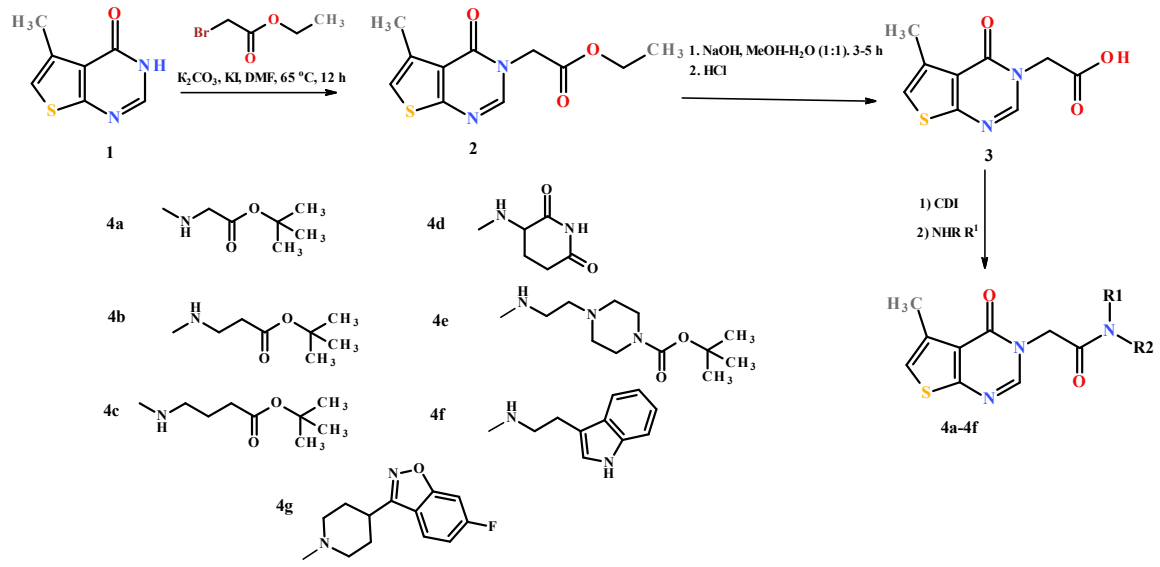

Fig. 2. Synthesis of target amides **4a-g** via conventional amide coupling strategy

For selecting structure candidates for *in vivo* studies in the scopolamine-induced mouse model of amnesia, acetylcholinesterase (AChE) in complex with Donepezil (PDB ID 7E3H) was chosen as the biomolecular target. Scopolamine, by blocking muscarinic receptors, induces an acute cholinergic deficit and reversible cognitive impairments. Inhibition of AChE increases acetylcholine levels and partially compensates for this deficit. Donepezil, in addition to its selective inhibition of AChE, is also suggested to influence β-amyloid (Aβ) metabolism *via* interaction with the peripheral anion site (PAS) of AChE, which participates in accelerating Aβ aggregation [49]. This makes the model suitable for evaluating both cholinergic and potential anti-amyloid effects.

Redocking of Donepezil into the AChE binding site successfully reproduced the key hydrogen-bonding pattern observed in the crystal structure, including the conventional H-bond between Phe295 (N) and the carbonyl-group of ligand, as well as several carbon–hydrogen bonds involving Tyr337, Ser293, and Tyr72. Additionally, the docking pose recovered the characteristic hydrophobic contacts and π–π interactions with Trp86, Trp286, Tyr341, Phe338, and Tyr337, confirming accurate recapitulation of the native binding mode.

All investigated ligands demonstrated high affinity toward the AChE inhibitor binding site, with predicted binding energies ranging from –8.4 to –12.5 kcal/mol, compared to –11.6 kcal/mol for Donepezil (Table 1).

Table 1

The results of the docking studies of the ligand **4a-g** and the native inhibitor to the active sites of AChE

Ligand	Affinity (kcal/mol)	Interaction with amino acid residues
Donepezil	–11.6	[a]Phe295, Tyr337, Ser293 [b] Tyr72, Tyr341(4), Trp286(3), Trp86(2), Tyr337, Phe338, Tyr124
4a	–8.7	[a]Tyr124 (3). His447 (2) [b]Trp86 (5), Trp286 (2), Phe297, Tyr341 [c] Trp86
4b	–9.1	[a]Tyr124 [b] Tyr341(2), Trp286(4), Trp86(4), Tyr337(2),, His447
4c	–8.4	[a] Tyr124 (3), Tyr341 [b] Tyr72, Tyr341, Trp286(5), Phe338, His447 (2)
4d	–10.2	[a]Tyr124 (3), Tyr341 Tyr337, Trp86 [b]Trp286 (5), Tyr341(3), Tyr337, Tyr72, TRP286
4e	–9.2	[a]Tyr124 (2), His447 [b]Trp286 (3), Trp86, Tyr341(3),Tyr72, GLY120. GLY121
4f	–10.9	[a]TYR133, TYR124(2), Asp74, Ser125 [b]Trp86 (5), Tyr341(3), Trp286 (3)
4g	–12.5	[a] TYR72, TYR133, TYR124(2) [b]Trp86 (3), Trp286 (3), Phe338, Tyr341, Tyr 337 [c] Trp286 (2)

Analysis of the conformational placement and interaction profiles suggests that compounds **4d, 4e, 4f,** and **4g** can adopt a stable, deeply embedded binding mode within the AChE active site. Using compound **4g** (6-fluoro-1,2-benzoxazol-3-yl)piperidinyl derivative) as an example, a comparison with Donepezil shows that both ligands preserve the key AChE "aromatic corridor," including π–π stacking with Trp86, Trp286, and Tyr341, as well as hydrophobic/π-alkyl contacts with Tyr337, Phe338, and Tyr341, indicating a similar overall binding orientation (Fig. 3).

At the same time, **4g** forms additional H-bonds (Tyr72, Tyr124, Tyr133), halogen interactions (Trp286), and a π–sulfur contact with Trp286, and exhibits a more favorable predicted binding energy (–12.5 vs –11.6 kcal/mol for Donepezil), indicating higher predicted affinity for AChE. Based on these structural and energetic advantages, compounds **4d**, **4e**, **4g** and **4f** were selected for subsequent *in vivo* evaluation in the scopolamine-induced mouse model.

The effects of compounds **4a–g** in the passive avoidance test in mice with scopolamine-induced amnesia are shown in Table 2. The baseline latency to enter the dark compartment for the vehicle control group averaged 66.2 seconds. After 24 hours, none of these animals entered the dark chamber within the 3-minute observation period, indicating 100% retention of the training criterion. In the scopolamine-induced amnesia group, the latency was significantly shorter compared to the vehicle control. After 24 hours, only 33% of these animals met the training criterion, demonstrating the amnestic effect of scopolamine. Although donepezil showed a tendency to prolong latency compared to the scopolamine-only group, it had minimal impact on reversing memory impairment. In the donepezil group, only 33% of animals achieved the training criterion on the first day, resulting in a modest anti-amnestic activity index of 13.6% after 24 hours.

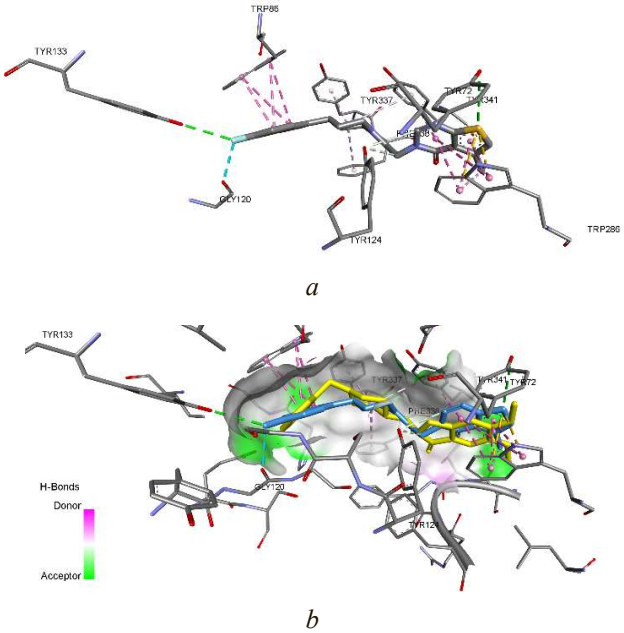

a

b

Fig. 3. Visualization: *a* – interaction of **4g** with amino acids of the active site of AChE inhibitors; *b* – conformations Donepezil (yellow structure) and the ligand **4g** (blue structure)

Table 2

The effect of the compounds **4** on passive avoidance test in mice with scopolamine-induced amnesia (PAT) (*M*±*SEM*, *Me* [Q25; Q75])

Group, *n*	Dose, mg/kg	Transfer latency, sec		% of animals which have reached the learning criterion, (%)	AA – antiamnestic activity index,%	The number of incomplete attempts to enter	
		training (1st day)	retention test (in 24 hours)			training (1st day)	after 24 hours
Vehicle control	–	66.2±20.6 75.0 [30.0; 103.0]	180.0±0.0 180.0 [180.0; 180.0]"	5/5 (100)	–	0.67±0.33 0.5 [0.0; 1.0]	1.0±0.68 0.0 [0.0; 1.5]
Amnesia control group (scopolamine)	1.5	23.0±7.27 22.5 [8.75; 37.0]	74.3±33.7 30.0 [17.75; 145.0]*	2/6 (33.3) ^^	–	0.33±0.33 0.0 [0.0; 0.0]	1.0±0.68 0.0 [0.0; 1.5]
Scopolamine + Donepezil	1.5 + 3.0	38.5±7.63 34.5 [30.25; 44.75]	98.33±31.17 96.00 [29.00; 169.00]*	2/6 (33.3) ^^	13.6	0.33±0.33 0.0 [0.0; 0.0]	3.67±1.63 2.5 [1.25; 4.5] "
Scopolamine +**4d**	1.5 + 2.64	45.2±15.5 30.0 [18.75; 63.75]	136.7±28.3 180.0 [103.5; 180.0]"	4/6 (66.7) ^	64.3	1.33±0.42 2.0 [0.5; 2.0]	3.0±1.13 3.0 [0.5; 5.5]
Scopolamine + **4e**	1.5 + 3.44	78.33±32.71 54.5 [12.5; 149.0]	123.5±35.77 180.00 [57.75; 180.0]"	4/6 (66.7) ^	–6.2	2.67±1.50 1.0 [0.0; 4.25]	2.17±0.91 2.0 [0.5; 2.75]
Scopolamine + **4f**	1.5 + 2.90	64.33±21.34 43.5 [39.0; 53.25]	145.0±25.0 180.0 [135.0; 180.0]	4/6 (66.7) ^	47.0	2.0±1.13 1.0 [0.0; 2.75]	2.0±0.89 2.0 [0.0; 2.0]
Scopolamine + **4g**	1.5 + 3.37	112.0±29.1# 123.0 [70.0; 173.75]	134.7±28.7 180.0 [82.5; 180.00]	4/6 (66.7) ^	36.3	2.83±0.65 3.5 [2.25; 4.0]	1.67±0.67 1.5 [0.25; 2.75]

*Note: significant relative to the vehicle control group: * – $p<0.05$ (Mann-Whitney criterion); ^ – $p<0.05$ ^^ – $p<0.01$ (Fisher Criterion); significant relative to the amnesia control group: # – $p<0.05$ (mann-whitney criterion); statistically significant differences within groups: " – $p<0.05$ (Wilcoxon signed-rank test).*

Compound **4g** significantly increased the latency to enter the dark chamber, with values 4.9-fold higher than in the amnesia control group ($p < 0.05$). After 24 hours, the latency remained slightly lower than that of the vehicle control group, without significant difference. The proportion of animals that achieved the training criterion in the **4g** group was 66.7%, and the anti-amnestic activity index reached 36.3%. Compounds **4d** and **4f** demonstrated moderate anti-amnestic effects, with activity levels of 64.3% and 47.0%, respectively. Compound **4e** did not significantly change memory performance (*AA* = 6.2%). In all other treated groups, latency times did not differ significantly from those observed in the vehicle control or amnesia control groups at baseline or after 24 h.

In the scopolamine amnesia group, the number of rearing decreased approximately fourfold compared to the vehicle control. This effect persisted for 24 h. Scopolamine also significantly reduced the number of fecal boli after 24 h (Table 3). This indicates a weakening of the vegetative support of emotional reactions. Donepezil also reduced baseline exploratory activity, but after 24 h it returned to the level of intact animals. The number of fecal boli remained significantly lower than in intact controls, which may reflect a reduction in anxiety. Administration of **4g** did not alter rearing counts relative to baseline; however, rearing was significantly higher than those in the scopolamine group. In the **4d** group, initial rearing counts were significantly reduced compared to the intact control. After 24 h, rearing values increased 13.7-fold, reaching levels comparable to the vehicle control. Compounds **4e** and **4f** produced only slight, non-significant changes in rearings, reaching values similar to the intact group. No significant changes were observed for other emotional or vegetative markers in these groups.

The effects of the tested compounds on coordination and balance were evaluated using the rotarod test after the PAT procedure, which had been preceded by scopolamine administration. The results were compared with those of the vehicle control group and the scopolamine-induced amnesia group (Table 4). In the scopolamine group, motor coordination was impaired, as reflected by nearly a twofold reduction in the time to fall compared with the vehicle control. Donepezil, as well as compounds **4e** and **4f**, produced a slight increase in fall latency, reaching values comparable to the control group. Administration of compounds **4g** and **4d** did not alter coordination, with fall latency remaining at the level observed in the scopolamine group.

The analgesic effect of the tested compounds was evaluated using the hot plate test, performed after the PAT and rotarod assessments. Since all animals received scopolamine prior to testing, results were compared between the donepezil-treated group and the scopolamine-only (amnesia control) group (Table 5). Scopolamine produced a statistically significant analgesic effect, increasing the latency of the nociceptive response by 3.9-fold compared with the vehicle control. Donepezil had minimal influence on nociceptive latency. Com-

pounds **4g** and **4f** showed a slight, non-significant tendency toward decreasing the latency period. Compounds **4d** and **4e** significantly reduced the latency compared with the amnesia control group.

Table 3

The effect of donepezil and the studied compounds on the on exploratory behavior, emotional reactions and their vegetative accompaniment in mice with scopolamine-induced amnesia in PAT ($M \pm$ SEM, Me [Q25; Q75])

Group, $n = 6$	Rearing		Auto grooming	
	Initial state	After 24 hours	Initial state	After 24 hours
Vehicle control	4.17±1.08 4.50 [3.25; 5.00]	5.83±2.30 3.00 [2.25; 9.75]	0.67±0.33 0.50 [0; 1.00]	0.83±0.31 1.00 [0.25;1.00]
Amnesia control group (scopolamine)	1.00±0.52 0.50 [0.00; 1.75]*	1.00±0.37 1.00 [0.25; 1.75]*	0.00±0.00 0 [0; 0]	0.17±0.17 0.00 [0; 0]
Scopolamine + Donepezil	1.00±0.52 0.50 [0; 1.75]*	5.00±3.25 1.00 [0.25; 6.25]	0.00±0.00 0 [0; 0]	0.50±0.34 0 [0; 0.75]
Scopolamine + **4d**	0.67±0.33 0.50 [0; 1.00]*	9.17±2.40 10.00 [5.25; 12.50]»	0.00±0.00 0 [0; 0]	0.50±0.22 0.50 [0; 1.00]
Scopolamine + **4e**	2.50±1.02 2.00 [1.00; 3.00]	4.50±2.43 2.00 [0.25; 6.75]	0.67±0.49 0 [0; 0.75]	0.83±0.31 1.00 [0.25;1.00]
Scopolamine + **4f**	1.83±1.33 0 [0; 2.25]	8.17±2.59 7.50 [2.75; 11.50]»	0.00±0.00 0 [0; 0]	0.50±0.34 0 [0; 0.75]
Scopolamine + **4g**	4.67±1.02 5.00 [3.25; 6.00]#	4.67±1.52 3.50 [2.25; 6.25]	0.50±0.34 0 [0; 0.75]	0.50±0.22 0.50 [0; 1.00]
	Fecal boli		Urinations	
Vehicle control	1.50±1.02 0 [0; 2.25]	3.17±0.83 3.50 [2.25; 4.00]	0.00±0.00 0 [0; 0]	0.17±0.17 0 [0; 0]
Amnesia control group (scopolamine)	0.00±0.00 0 [0; 0]	0.17±0.17 0 [0; 0]**	0.00 ± 0.00 0 [0; 0]	0.00±0.00 0 [0; 0]
Scopolamine + Donepezil	0.00±0.00 0 [0; 0]	0.50±0.34 0 [0; 0.75]*	0.00±0.00 0 [0; 0]	0.00±0.00 0 [0; 0]
Scopolamine + **4d**	0.00±0.00 0 [0; 0]	1.50±0.56 1.50 [0.25; 2.75]	0.00±0.00 0 [0; 0]	0.00±0.00 0 [0; 0]
Scopolamine + **4e**	0.00±0.00 0 [0; 0]	2.50±0.96 2.50 [0.50; 3.75]	0.00±0.00 0 [0; 0]	0.00±0.00 0 [0; 0]
Scopolamine + **4f**	0.00±0.00 0 [0; 0]	0.83±0.83 0 [0; 0]	0.00±0.00 0 [0; 0]	0.00±0.00 0 [0; 0]
Scopolamine + **4g**	0.00±0.00 0 [0; 0]	2.33±1.05 2.00 [0; 4.75]	0.00±0.00 0 [0; 0]	0.00±0.00 0 [0; 0]

*Note: significant relative to the vehicle control group: * – $p < 0.05$ (Mann-Whitney criterion); significant relative to the amnesia control group (scopolamine): # – $p < 0.05$ (Mann-Whitney criterion); statistically significant differences within groups: " – $p < 0.05$ (Wilcoxon signed-rank test).*

Table 4

The effect of Donepezil and the tested compounds on coordination and balance e of mice in rotarod test (M ± SEM, Me [Q25; Q75])

Group, $n = 6$)	$M \pm m$	Latency time, sec	The number of animals that fall form the rod, %			
			less than 30 sec	before 1 min	before 2 min	more than 2 min
1	2	3	4	5	6	7
Vehicle control	111.67± 8.33	120 [120; 120]	0	0	16.7	83.3
Amnesia control group (scopolamine)	63.17± 17.75	52.5 [31;98]**	33.3^	33.3^	16.7	16.7^^

Continuation of Table 4

1	2	3	4	5	6	7
Scopolamine + Donepezil	93.83± 13.80	110 [67;120]	0	33.3^	16.7	50.0
Scopolamine + **4d**	60.83± 19.17	42.5 [26.5; 101.2]*	33.3^	33.3^	0	33.3^
Scopolamine + **4e**	98.00± 14.38	120 [81; 120]	0	16.7	16.7	66.7
Scopolamine + **4f**	90.33± 15.58	107 [66.2; 120]	0	33.3^	16.7	50.0
Scopolamine + **4g**	67.33± 17.27	50.5 [38.7; 105]*	16.7	50.0^^	0	33.3^

*Note: significant relative to the vehicle control group: * – $p < 0.05$, ** – $p < 0.01$ Mann-Whitney criterion); ^ – $p < 0.05$, ^^ – $p < 0.01$ (Fisher Criterion).*

Table 5

Influence of Donepezil and the tested compounds on the nociceptive pain reaction in mice in Hot-plate test (M ± SEM, Me [Q25; Q75])

Group, $n = 6$	Latent time of the hind paw licking, sec.		The number of animals, which had nociceptive reaction,%				
	$M \pm m$	Me [Q25; Q75]	less 10 sec.	less 15 sec.	less 30 sec.	less 1 min	more 1 min.
Vehicle control	13.20 ± 2.75	10.5 [9.93; 12.88]	50.0	33.3	16.7	0	0
Amnesia control group (scopolamine)	50.87 ± 5.88**	60 [42.6; 60]**	0^^	0^	16.7	16.7	66.7^^
Scopolamine + Donepezil	45.40 ± 5.78	46.45 [37; 57.5]*	0^^	0^	16.7	50.0^^	33.3^
Scopolamine + **4d**	31.40 ± 6.41	26 [21.05;35.4] *#	0^^	0^	50.00%	33.3^	16.7
Scopolamine + **4e**	29.23 ± 5.16	27.95 [22.8; 33.90] *#	0^^	16.7	50.0	33.3^	0
Scopolamine +**4f**	35.60 ± 6.33*	36.4 [26.13;41]*	0^^	0^	33.3	50.0^^	16.7
Scopolamine +**4g**	31.37 ± 6.64	28.2 [19.9; 36.03]*	0^^	0^	50.0	33.3^	16.7

*Note: significant relative to the vehicle control group: * – $p < 0.05$, ** – $p < 0.01$ (Mann-Whitney criterion); ^ – $p < 0.05$, ^^ – $p < 0.01$ (Fisher Criterion); significant relative to the amnesia control group (scopolamine): # – $p < 0.05$ (Mann-Whitney criterion).*

5. Discussion

The present study demonstrated that the thienopyrimidine scaffold is well suited for efficient functionalization aimed at generating hybrid molecules incorporating biogenic fragments. Optimization of the N-alkylation step played a key role in the synthetic scheme: the addition of potassium iodide as a reagent of *in situ* Finkelstein reaction accelerated the interaction and increased the regioselectivity toward formation of the desired N-alkylated isomer. The improved crystallization procedure further facilitated selective isolation of the target product. Together, these optimizations enabled a reproducible access to the key intermediate 5-methyl-4-oxothieno[2,3-d]pyrimidin-3(4*H*)-yl)acetic acid **3** which served as the basis for constructing the hybrid structures. Hydrolysis of the obtained ester **2** in a methanol-water mixture proved to be an optimal approach, providing acid **3** in high purity and ensuring its suitability for direct use in the subsequent amide-coupling stage. The synthesis of hybrid molecules **4** by peptide-like coupling methods confirmed the functional versatility of the chosen synthetic strategy. Despite the low solubility of the acid **3** in 1,4-dioxane, its rapid *in situ* conversion into the corresponding imidazolide ensured good solubility and high reactivity. The use of equimolar amounts of triethylamine promoted effective activation of amino acid esters and amines, yielding the amide products under mild conditions.

An additional advantage of the developed method was the simplicity of isolating the target compounds. Overall, the optimized sequence – selective N-alkylation, controlled hydrolysis, and efficient amide coupling proved to be a reliable approach for obtaining a diverse set of thienopyrimidine hybrids incorporating both biogenic and synthetic components.

According to the molecular docking results several structures **4d** (glutamic acid imide derivative), **4f** (tryptamine derivative) and **4g** (6-fluoro-1,2-benzoxazol-3-yl) piperidinyl derivative demonstrated the most favorable binding energies and formed an extended network of hydrogen, halogen, and π-interactions within the AChE "aromatic gorge" (Trp86, Trp286, Tyr337, Tyr341, Phe338), ensuring deeper and more stable accommodation in the active site [48]. These same compounds also exhibited the strongest pro-cognitive effects in the scopolamine-induced amnesia model. Notably, compound **4g**, which had the best binding energy (–12.5 kcal/mol), showed activity comparable to or exceeding that of Donepezil, illustrating a correlation between the in silico and *in vivo* findings. In contrast, amino-acid linkers derived from glycine, alanine, and aminobutyric acid did not contribute significantly to conformational stabilization, whereas the

tert-butyl substituent (in compound **4e**) provided additional hydrophobic contacts. The lack of the expected *in vivo* activity for derivative **4e** may be attributed to hydrolysis or metabolic instability.

It should be noted that Donepezil, despite existing reports of its anti-amnestic [49], anxiolytic [50], and analgesic [51] properties, did not exhibit any of these effects in our experiment. This may indicate that such effects are unstable or highly dependent on specific experimental conditions. The compounds **4g**, **4d** and **4f** in the experiment showed moderate anti-amnestic properties. At the same time, the results of behavioral testing demonstrate that compound **4g** significantly increases the initial latency during the information assimilation phase. This indicates an anxiolytic-like effect, which requires further in-depth studies. The improvement in the proportion of animals meeting the training criterion, together with a moderate anti-amnestic index, indicates that **4g** may support processes associated with mnemonic retention. Although the effect after 24 hours did not reach the level of the vehicle control, the overall pattern of responses points to a partial preservation of memory function under cholinergic blockade. The marked reduction of exploratory activity (rearing) in the scopolamine group aligns with known effects of muscarinic antagonists on emotional processing. The normalization of rearing behavior after in the **4d** group suggests potential anxiolytic involvement, which complements its performance in the PAT test. Compounds **4e** and **4f** showed little effect on rearing or vegetative markers, indicating a limited impact on emotional or autonomic components. All the tested compounds do not have analgesic properties. Overall, the combined behavioral findings indicate that the tested hybrid thienopyrimidine derivatives exert differential CNS activity, with **4g** showing the most pronounced composite profile involving modulation of anxiety-related and mnemonic functions, while **4d** and **4f** provide moderate support for memory retention.

The rotarod data confirm that scopolamine administration induces measurable motor impairment, which aligns with its known central and peripheral effects on neuromuscular coordination [52]. The partial restoration of fall latency observed for donepezil, compounds **4e** and **4f** suggests that these molecules may counteract scopolamine-induced deficits to some extent, potentially through cholinergic modulation or other CNS-mediated mechanisms. In contrast, compounds **4g** and **4d** did not improve coordination, indicating limited involvement in pathways governing motor control.

The hot plate test confirmed that scopolamine alters pain responsiveness, which aligns with reports describing its modulatory influence on central cholinergic pathways involved in nociception [53]. The absence of an effect in the donepezil-treated group indicates that cholinesterase inhibition does not counteract scopolamine-induced changes in thermal pain sensitivity under these experimental conditions. None of the tested compounds exhibited analgesic properties in the hot plate assay.

Practical relevance. The results of this study have practical relevance for the development of novel therapeutic agents aimed at mitigating cognitive impairment associated with cholinergic dysfunction. The demonstrated approach also highlights the value of integrating pharmacophore modeling, docking, and behavioral screening as an efficient workflow for discovering new candidates for the treatment of memory deficits.

Study limitations. Several limitations of the present study should be acknowledged. First, molecular docking provides only a static approximation of ligand-AChE interactions and does not account for dynamic effects. It is necessary to expand the molecular docking on a number of targets of anti-amnestic, anxiolytic effect, and nociceptive reactions. Second, the *in vivo* evaluation was conducted using an acute scopolamine-induced amnesia model, which reflects reversible cholinergic dysfunction but does not fully represent the multifactorial nature of chronic neurodegenerative conditions such as Alzheimer's disease. Third, pharmacokinetic properties, metabolic stability, and BBB penetration were not directly assessed, which may explain discrepancies between predicted affinity and behavioral outcomes. Finally, the behavioral battery was limited to memory, anxiety, effects on motor coordination and nociception, and future studies should incorporate additional cognitive functions, emotional and nociceptive responses, and their biochemical markers to obtain a more complete pharmacological comprehensive characterization of the compounds.

Prospects for further research. Further structural optimization of the selected compounds, guided by the identified interaction patterns, together with more in-depth preclinical studies, may lead to the development of derivatives with enhanced neuroprotective properties.

6. Conclusions

The rational design, synthesis, and structural characterization of new AChE-targeted derivatives, combined with *in silico* simulations and subsequent *in vivo* validation, enabled the identification of several thieno[2,3-d]pyrimidine derivatives with moderate anti-amnestic properties in the scopolamine-induced amnesia model, highlighting their potential as promising structures for further optimization. The methods for synthesizing the intermediates and target hybrids of 5-methylthieno[2,3-d]pyrimidin-4(3H)-one *via* amide coupling were optimized. The variation of pharmacophoric elements made it possible to investigate the influence of different substituents on affinity and biological activity. A positive contribution was identified for the glutamic acid imide moiety (**4d**), the tryptamine fragment (**4f**), and the 6-fluoro-1,2-benzoxazol-3-yl)piperidinyl group (**4g**). The integrated approach combining structural design, synthesis, docking, and a series of behavioral studies proved effective for identifying new potential modulators of the cholinergic system, particularly derivative **4g**, which combines anti-amnestic and anxiolytic-like properties. The results obtained provide a foundation for further structural optimization of the most promising compounds and for expanded preclinical investigations of their psychotropic and neuroprotective activity.

Conflict of interests

The authors declare that they have no conflict of interest in relation to this research, whether financial, personal, authorship or otherwise, that could affect the research and its results presented in this article.

Funding

The research was funded by the Ministry of Health of Ukraine at the expense of the State Budget in the framework # 2301020 "Scientific and scientific-technical activity in the field of health protection" on the topic «Molecular modelling and synthesis of innovative pyrimidine derivatives as promising agents for the treatment of neurodegenerative diseases» (State registration number: 0124U002006. Order of the Ministry of Health of Ukraine of January 16, 2024, No. 82)

Use of artificial intelligence

The authors confirm that they did not use artificial intelligence technologies when creating the current work.

Acknowledgement

The authors acknowledge Enamine Ltd. for the support of synthetic experiments and measurement of ^{1}H, ^{13}C NMR and LC-MS spectra of the obtained substances.

Authors' contributions

Rita Saifudinova: Investigation, Data Curation, Writing – Original Draft. **Sergiy Vlasov**: Project Administration, Data Curation, Validation, Writing – Review & Editing; **Hanna Severina** (*Corresponding author*): Conceptualization, Supervision, Writing – Review & Editing, Funding Acquisition; **Georgiy Yakovenko**: Methodology, Resources, Data Curation, Visualization; **Andrii Khairulin**: Methodology, Formal Analysis, Software; **Dmytro Kyrylov**: Investigation, Data Curation, Writing – Original Draft; **Mykyta Hutorka**: Investigation, Data Curation, Visualization; **Sergii Shtrygol'**: Conceptualization, Supervision, Validation, Writing – Review & Editing; **Victoriya Georgiyants**: Supervision, Validation, Writing – Review & Editing.

References

1. Arlt, S. (2013). Non-Alzheimer's disease – related memory impairment and dementia. Dialogues in Clinical Neuroscience, 15 (4), 465–473. https://doi.org/10.31887/dcns.2013.15.4/sarlt

2. Morais, R., Pires, R., Jesus, T., Lemos, R., Duro, D., Lima, M. et al. (2024). Cognitive Impairment in Neurodegenerative Diseases: A Trans-Diagnostic Approach Using a Lesion-Symptom Mapping Analysis. Neuroscience. https://doi.org/10.2139/ssrn.5030776

3. Pentkowski, N. S., Rogge-Obando, K. K., Donaldson, T. N., Bouquin, S. J., Clark, B. J. (2021). Anxiety and Alzheimer's disease: Behavioral analysis and neural basis in rodent models of Alzheimer's-related neuropathology. Neuroscience & Biobehavioral Reviews, 127, 647–658. https://doi.org/10.1016/j.neubiorev.2021.05.005

4. Blanton, H., Reddy, P. H., Benamar, K. (2023). Chronic pain in Alzheimer's disease: Endocannabinoid system. Experimental Neurology, 360, 114287. https://doi.org/10.1016/j.expneurol.2022.114287

5. Aillaud, I., Kaniyappan, S., Chandupatla, R. R., Ramirez, L. M., Alkhashrom, S., Eichler, J. et al. (2022). A novel D-amino acid peptide with therapeutic potential (ISAD1) inhibits aggregation of neurotoxic disease-relevant mutant Tau and prevents Tau toxicity in vitro. Alzheimer's Research & Therapy, 14 (1). https://doi.org/10.1186/s13195-022-00959-z

6. Ullah, R., Jo, M. H., Riaz, M., Alam, S. I., Saeed, K., Ali, W. et al. (2020). Glycine, the smallest amino acid, confers neuroprotection against d-galactose-induced neurodegeneration and memory impairment by regulating c-Jun N-terminal kinase in the mouse brain. Journal of Neuroinflammation, 17 (1). https://doi.org/10.1186/s12974-020-01989-w

7. Salek, R. M., Xia, J., Innes, A., Sweatman, B. C., Adalbert, R., Randle, S. et al. (2010). A metabolomic study of the CRND8 transgenic mouse model of Alzheimer's disease. Neurochemistry International, 56 (8), 937–947. https://doi.org/10.1016/j.neuint.2010.04.001

8. Li, H., Ye, D., Xie, W., Hua, F., Yang, Y., Wu, J. et al. (2018). Defect of branched-chain amino acid metabolism promotes the development of Alzheimer's disease by targeting the mTOR signaling. Bioscience Reports, 38 (4). https://doi.org/10.1042/bsr20180127

9. Kazim, S. F., Iqbal, K. (2016). Neurotrophic factor small-molecule mimetics mediated neuroregeneration and synaptic repair: emerging therapeutic modality for Alzheimer's disease. Molecular Neurodegeneration, 11 (1). https://doi.org/10.1186/s13024-016-0119-y

10. Akazawa, N., Hamasaki, A., Tanahashi, K., Kosaki, K., Yoshikawa, T., Myoenzono, K., Maeda, S. (2018). Lactotripeptide ingestion increases cerebral blood flow velocity in middle-aged and older adults. Nutrition Research, 53, 61–66. https://doi.org/10.1016/j.nutres.2018.03.009

11. Min, L.-J., Kobayashi, Y., Mogi, M., Tsukuda, K., Yamada, A., Yamauchi, K. et al. (2017). Administration of bovine casein-derived peptide prevents cognitive decline in Alzheimer disease model mice. PLOS ONE, 12 (2), e0171515. https://doi.org/10.1371/journal.pone.0171515

12. Singh, Y. P., Kumar, H. (2023). Tryptamine: A privileged scaffold for the management of Alzheimer's disease. Drug Development Research, 84 (8), 1578–1594. Portico. https://doi.org/10.1002/ddr.22111

13. Wu, Y.-L., Yoshida, M., Emoto, H., Ishii, H., Koga, K., Tanaka, M. (2000). Effects of Acute and Chronic Administration of MCI-225, a New Selective Noradrenaline Reuptake Inhibitor With 5-HT3 Receptor Blocking Action, on Extracellular Noradrenaline Levels in the Hypothalamus of Stressed Rats. Japanese Journal of Pharmacology, 83 (1), 31–38. https://doi.org/10.1016/s0021-5198(19)30624-9

14. Galvani, F., Cammarota, M., Vacondio, F., Rivara, S., Boscia, F. (2024). Protective Activity of Melatonin Combinations and Melatonin-Based Hybrid Molecules in Neurodegenerative Diseases. Journal of Pineal Research, 76 (8). https://doi.org/10.1111/jpi.70008

15. Babazadeh, A., Vahed, F. M., Liu, Q., Siddiqui, S. A., Kharazmi, M. S., Jafari, S. M. (2023). Natural Bioactive Molecules as Neuromedicines for the Treatment/Prevention of Neurodegenerative Diseases. ACS Omega, 8 (4), 3667–3683. https://doi.org/10.1021/acsomega.2c06098

16. Singh, A. A., Khan, F., Song, M. (2025). Alleviation of Neurological Disorders by Targeting Neurodegenerative-Associated Enzymes: Natural and Synthetic Molecules. International Journal of Molecular Sciences, 26 (10), 4707. https://doi.org/10.3390/ijms26104707

17. Ortiz, C. J. C., Damasio, C. M., Pruccoli, L., Nadur, N. F., de Azevedo, L. L., Guedes, I. A. et al. (2020). Cinnamoyl-N-Acylhydrazone-Donepezil Hybrids: Synthesis and Evaluation of Novel Multifunctional Ligands Against Neurodegenerative Diseases. Neurochemical Research, 45 (12), 3003–3020. https://doi.org/10.1007/s11064-020-03148-2

18. Fotopoulos, I., Pontiki, E., Hadjipavlou-Litina, D. (2024). Pharmacochemical Study of Multitarget Amino Acids' Hybrids: Design, Synthesis, In vitro, and In silico Studies. Medicinal Chemistry, 20 (7), 709–720. https://doi.org/10.2174/0115734064279653240125081042

19. Fontana, I. C., Souza, D. G., Souza, D. O., Gee, A., Zimmer, E. R., Bongarzone, S. (2023). A Medicinal Chemistry Perspective on Excitatory Amino Acid Transporter 2 Dysfunction in Neurodegenerative Diseases. Journal of Medicinal Chemistry, 66 (4), 2330–2346. https://doi.org/10.1021/acs.jmedchem.2c01572

20. Paul, S. S., Biswas, G. (2021). A Mini-Review on the Effectiveness of Peptoids as Therapeutic Interventions against Neurodegenerative Diseases. Current Protein & Peptide Science, 22 (7), 526–533. https://doi.org/10.2174/1389203722666210615125852

21. Hatvate, N. T., Shevkar, T. S., Akolkar, H.; Kulkarni, S., Akolkar, H., Khedkar, V., Darekar, N. (Eds.) (2024). Thienopyrimidines Exploring the Chemistry and Bioactivity. Examining Biological Relevance of Fused S-Heterocycles. IGI Global Scientific Publishing, 221–272. https://doi.org/10.4018/979-8-3693-7520-4.ch008

22. Kassab, A. E., Gedawy, E. M., Sayed, A. S. (2024). Fused thiophene as a privileged scaffold: A review on anti-Alzheimer's disease potentials via targeting cholinesterases, monoamine oxidases, glycogen synthase kinase-3, and Aβ aggregation. International Journal of Biological Macromolecules, 265, 131018. https://doi.org/10.1016/j.ijbiomac.2024.131018

23. Eissa, K. I., Kamel, M. M., Mohamed, L. W., Doghish, A. S., Alnajjar, R., Al-Karmalawy, A. A., Kassab, A. E. (2023). Design, synthesis, and biological evaluation of thienopyrimidine derivatives as multifunctional agents against Alzheimer's disease. Drug Development Research, 84 (5), 937–961. https://doi.org/10.1002/ddr.22064

24. DDP-225. DrugBank. Available at: https://go.drugbank.com/drugs/DB05642 Last accessed: 12.06.2025

25. Banks, W. A., Rhea, E. M., Reed, M. J., Erickson, M. A. (2024). The penetration of therapeutics across the blood-brain barrier: Classic case studies and clinical implications. Cell Reports Medicine, 5 (11), 101760. https://doi.org/10.1016/j.xcrm.2024.101760

26. Ahunovych, V., Klipkov, A. A., Bugera, M., Tarasenko, K., Trofymchuk, S., Razhyk, B. et al. (2024). CF3-Cyclobutanes: Synthesis, Properties, and Evaluation as a Unique tert-Butyl Group Analogue. JACS Au, 4 (11), 4507–4517. https://doi.org/10.1021/jacsau.4c00864

27. Novotná, K., Tenora, L., Prchalová, E., Paule, J., Alt, J., Veeravalli, V. et al. (2023). Discovery of tert-Butyl Ester Based 6-Diazo-5-oxo-l-norleucine Prodrugs for Enhanced Metabolic Stability and Tumor Delivery. Journal of Medicinal Chemistry, 66 (22), 15493–15510. https://doi.org/10.1021/acs.jmedchem.3c01681

28. Salga, S. M., Ali, H. M., Abdullah, M. A., Abdelwahab, S. I., Wai, L. K., Buckle, M. J. C. et al. (2011). Synthesis, Characterization, Acetylcholinesterase Inhibition, Molecular Modeling and Antioxidant Activities of Some Novel Schiff Bases Derived from 1-(2-Ketoiminoethyl)piperazines. Molecules, 16 (11), 9316–9330. https://doi.org/10.3390/molecules16119316

29. 6-Fluoro-3-(4-piperidinyl)-1,2-benzisoxazole hydrochloride. Ossila. Available at: https://www.ossila.com/products/6-fluoro-3-4-piperidinyl-1-2-benzisoxazole-hydrochloride Last accessed: 17.06.2025

30. Cen, L., Wu, Y., He, M., Huang, J., Ren, W., Liu, B. et al. (2025). Discovery and Optimization of Novel Apo-IDO1 Inhibitors by a Pharmacophore-Based Structural Simplification Strategy. Journal of Medicinal Chemistry, 68 (6), 6633–6655. https://doi.org/10.1021/acs.jmedchem.5c00034

31. Shaker, M., Elhamifar, D. (2020). Pd-containing IL-based ordered nanostructured organosilica: A powerful and recoverable catalyst for Sonogashira reaction. Tetrahedron Letters, 61 (47), 152481. https://doi.org/10.1016/j.tetlet.2020.152481

32. Bassetto, M., Leyssen, P., Neyts, J., Yerukhimovich, M. M., Frick, D. N., Brancale, A. (2016). Computer-aided identification, synthesis and evaluation of substituted thienopyrimidines as novel inhibitors of HCV replication. European Journal of Medicinal Chemistry, 123, 31–47. https://doi.org/10.1016/j.ejmech.2016.07.035

33. Lou, J., Liu, Z., Li, Y., Zhou, M., Zhang, Z., Zheng, S. et al. (2011). Synthesis and anti-tumor activities of N′-benzylidene-2-(4-oxothieno[2,3-d]pyrimidin-3(4H)-yl)acetohydrazone derivatives. Bioorganic & Medicinal Chemistry Letters, 21 (22), 6662–6666. https://doi.org/10.1016/j.bmcl.2011.09.061

34. Protein Data Bank. Available at: https://www.rcsb.org/ Last accessed: 15.08.2025

35. Dileep, K. V., Ihara, K., Mishima-Tsumagari, C., Kukimoto-Niino, M., Yonemochi, M., Hanada, K. et al. (2022). Crystal structure of human acetylcholinesterase in complex with tacrine: Implications for drug discovery. International Journal of Biological Macromolecules, 210, 172–181. https://doi.org/10.1016/j.ijbiomac.2022.05.009

36. Directive 2010/63/EU of the European Parliament and of the Council of 22 September 2010 on the protection of animals used for scientific purposes (2010). Official Journal of the European Union. Available at: https://eur-lex.europa.eu/LexUriServ/LexUriServ.do?uri = OJ:L:2010:276:0033:0079:en:PDF

37. Housing and husbandry: Mouse (2024). National Centre for the Replacement, Refinement and Reduction of Animals in Research. Available at: https://nc3rs.org.uk/3rs-resources/housing-and-husbandry-mouse

38. Pellegrini, C., D'Antongiovanni, V., Fornai, M., Duranti, E., Baldacci, F., Bernardini, N. et al. (2021). Donepezil improves vascular function in a mouse model of Alzheimer's disease. Pharmacology Research & Perspectives, 9 (6). https://doi.org/10.1002/prp2.871

39. Vogel, H. G. (2007). Drug Discovery and Evaluation: Pharmacological Assays. Berlin Heidelberg New York: Springer-Verlag.

40. Semenets, A. P., Suleiman, M. M., Fedosov, A. I., Shtrygol, S. Y., Havrylov, I. O., Mishchenko, M. V. et al. (2022). Synthesis, docking, and biological evaluation of novel 1-benzyl-4-(4-(R)-5-sulfonylidene-4,5-dihydro-1H-1,2,4-triazol-3-yl)pyrrolidin-2-ones as potential nootropic agents. European Journal of Medicinal Chemistry, 244, 114823. https://doi.org/10.1016/j.ejmech.2022.114823

41. Podolsky, I., Shtrygol', S. (2019). The behavioral study of the effects of atristamine on the serotonin, dopamine and norepinephrine neurotransmitter systems in mice. Farmacia, 67 (2), 296–304. https://doi.org/10.31925/farmacia.2019.2.14

42. Havrylov, I., Shtrygol', S. (2021). Investigation of the effect of a modified fragment of neuropeptide Y on memory phases and extrapolation escape of animals. Česká a Slovenská Farmacie, 70 (3), 91–99. https://doi.org/10.5817/csf2021-3-91

43. Bloch, S., Belzung, C.; Harro, J. (Ed.) (2023). The Light–Dark Box Test in the Mouse. Psychiatric Vulnerability, Mood, and Anxiety Disorders. New York: Humana, 31–41. https://doi.org/10.1007/978-1-0716-2748-8_3

44. Takao, K., Miyakawa, T. (2006). Light/dark Transition Test for Mice. Journal of Visualized Experiments, 1. https://doi.org/10.3791/104

45. Hock, F. J. (Ed.) (2014). Drug discovery and evaluation: Pharmacological assays. Berlin, Heidelberg: Springer. https://doi.org/10.1007/978-3-642-27728-3

46. Moser, V. C. (2010). Functional Assays for Neurotoxicity Testing. Toxicologic Pathology, 39 (1), 36–45. https://doi.org/10.1177/0192623310385255

47. Hunskaar, S., Berge, O.-G., Hole, K. (1986). A modified hot-plate test sensitivie to mild analgesics. Behavioural Brain Research, 21 (2), 101–108. https://doi.org/10.1016/0166-4328(86)90088-4

48. Grabowska, W., Bijak, M., Szelenberger, R., Gorniak, L., Podogrocki, M., Harmata, P., Cichon, N. (2025). Acetylcholinesterase as a Multifunctional Target in Amyloid-Driven Neurodegeneration: From Dual-Site Inhibitors to Anti-Agregation Strategies. International Journal of Molecular Sciences, 26 (17), 8726. https://doi.org/10.3390/ijms26178726

49. Zhang, J., Wang, J., Zhou, G.-S., Tan, Y.-J., Tao, H.-J., Chen, J.-Q. et al. (2019). Studies of the Anti-amnesic Effects and Mechanisms of Single and Combined Use of Donepezil and Ginkgo Ketoester Tablet on Scopolamine-Induced Memory Impairment in Mice. Oxidative Medicine and Cellular Longevity, 2019, 1–16. https://doi.org/10.1155/2019/8636835

50. Papp, M., Gruca, P., Lason-Tyburkiewicz, M., Willner, P. (2016). Antidepressant, anxiolytic and procognitive effects of rivastigmine and donepezil in the chronic mild stress model in rats. Psychopharmacology, 233 (7), 1235–1243. https://doi.org/10.1007/s00213-016-4206-0

51. Selvy, M., Mattévi, C., Dalbos, C., Aissouni, Y., Chapuy, E., Martin, P.-Y. et al. (2022). Analgesic and preventive effects of donepezil in animal models of chemotherapy-induced peripheral neuropathy: Involvement of spinal muscarinic acetylcholine M2 receptors. Biomedicine & Pharmacotherapy, 149, 112915. https://doi.org/10.1016/j.biopha.2022.112915

52. Pelsőczi, P., Lévay, G. (2017). Effect of Scopolamine on Mice Motor Activity, Lick Behavior and Reversal Learning in the IntelliCage. Neurochemical Research, 42 (12), 3597–3602. https://doi.org/10.1007/s11064-017-2408-4

53. Montigné, E., Balayssac, D. (2023). Exploring Cholinergic Compounds for Peripheral Neuropathic Pain Management: A Comprehensive Scoping Review of Rodent Model Studies. Pharmaceuticals, 16 (10), 1363. https://doi.org/10.3390/ph16101363

Received 21.10.2025
Received in revised form 25.11.2025
Accepted 11.12.2025
Published 30.12.2025

Rita Saifudinova, PhD Student, Department of Pharmaceutical Chemistry, National University of Pharmacy, H. Skovorody str., 53, Kharkiv, Ukraine, 61002, Head of Department, Pharmaceutical Department, Cherkasy Medical Academy, Khreshchatyk str, 215, Cherkasy, Ukraine, 18001

Hanna Severina*, Doctor of Pharmaceutical Science, Professor, Department of Pharmaceutical Chemistry, National University of Pharmacy, H. Skovorody str., 53, Kharkiv, Ukraine, 61002

Sergiy Vlasov, Doctor of Pharmaceutical Sciences, Professor, Department of Supramolecular Chemistry, Taras Shevchenko National University of Kyiv, Volodymyrska str., 60, Ukraine, Kyiv, 01033, Enamine Ltd., Winston Churchill str., 78, Kyiv, Ukraine, 02094

Yakovenko Georgiy, PhD, Chemical Faculty, Taras Shevchenko National University of Kyiv, Volodymyrska str., 60, Ukraine, Kyiv, 01033, Enamine Ltd., Winston Churchill str., 78, Kyiv, Ukraine, 02094

Andrii Khairulin, PhD, Chemical Faculty, Taras Shevchenko National University of Kyiv, Volodymyrska str., 60, Ukraine, Kyiv, 01033, Enamine Ltd., Winston Churchill str., 78, Kyiv, Ukraine, 02094

Dmytro Kyrylov, Department of Pharmacology and Clinical Pharmacy, National University of Pharmacy, H. Skovorody str., 53, Kharkiv, Ukraine, 61002

Mykyta Hutorka, Department of Pharmacology and Clinical Pharmacy, National University of Pharmacy, H. Skovorody str., 53, Kharkiv, Ukraine, 61002

Sergii Shtrygol', Doctor of Medical Sciences, Professor, Department of Pharmacology and Clinical Pharmacy, National University of Pharmacy, H. Skovorody str., 53, Kharkiv, Ukraine, 61002

Victoriya Georgiyants, Doctor of Pharmaceutical Sciences, Professor, Head of Department, Department of Pharmaceutical Chemistry, National University of Pharmacy, H. Skovorody str., 53, Kharkiv, Ukraine, 61002

***Corresponding author**: Hanna Severina, e-mail: severina.ai@ukr.net*